


Page Proof Instructions and Queries

Journal Title: TIM
Article Number: 708833

Greetings, and thank you for publishing with SAGE. We have prepared this page proof for your review. Please respond to each of the below queries by digitally marking this PDF using Adobe Reader (free at <https://get.adobe.com/reader>).

Please use *only* the circled tools to indicate your requests and responses, as edits via other tools/methods are not compatible with our software. To ask a question or request a formatting change (such as italics), please click the  tool and then choose “Text Callout.” To access the necessary tools, choose “Comment” from the right-side menu.



Sl. No.	Query
	GQ: Please confirm that all author information, including names, affiliations, sequence, and contact details, is correct.
	GQ: Please review the entire document for typographical errors, mathematical errors, and any other necessary corrections; check headings, tables, and figures.
	GQ: Please ensure that you have obtained and enclosed all necessary permissions for the reproduction of art works (e.g. illustrations, photographs, charts, maps, other visual material, etc.) not owned by yourself. please refer to your publishing agreement for further information.
	GQ: Please note that this proof represents your final opportunity to review your article prior to publication, so please do send all of your changes now.
	GQ: Please confirm that the funding and conflict of interest statements are accurate.
1	AQ: Huda et al., 2011? Please add to References
2	AQ: Full definition?
3	AQ: evidents correct here?
4	AQ: Other authors' names?
5	AQ: date and location of conference? Publisher's location and name?
6	AQ: date and location of conference? Publisher's location and name?
7	AQ: date and location of conference? Publisher's location?
8	AQ: date and location of conference? Publisher's location?
9	AQ: Volume?
10	AQ: Volume?
11	AQ: Publisher's location?
12	AQ: date and location of conference? Publisher's location and name?
13	AQ: date and location of conference? Publisher's location and name?
14	AQ : Publisher's location?
15	AQ: date and location of conference? Publisher's location and name?
16	AQ: date and location of conference? Publisher's location and name?

Geometric analysis-based trajectory planning and control for underactuated capsule systems with viscoelastic property

Transactions of the Institute of
Measurement and Control
1–12

© The Author(s) 2017

Reprints and permissions:

sagepub.co.uk/journalsPermissions.nav

DOI: 10.1177/0142331217708833

journals.sagepub.com/home/tim



Pengcheng Liu¹, Hongnian Yu¹ and Shuang Cang²

Abstract

This paper proposes a novel geometric analysis-based trajectory planning approach for underactuated capsule systems with viscoelastic property. The idea is to reduce complexity and to characterize coupling by imposing a harmonic drive and then to compute the dynamics projection onto a hyper-manifold, such that the issue of trajectory planning is converted into geometric analysis and trajectory optimization. The objective is to obtain optimal locomotion performance in terms of tracking error, average capsule speed and energy efficacy. Firstly, an analytical two-stage velocity trajectory is given based on control indexes and dynamic constraints. A locomotion-performance index is then proposed and evaluated to identify the optimal viscoelastic parameters. The trajectory is optimally parameterized through rigorous analysis. A nonlinear tracking controller is designed using collocated partial feedback linearization. For the sake of efficiency in progression and energy, the proposed method provides a novel approach in characterizing and planning motion trajectory for underactuated capsule systems such that the optimal locomotion can be achieved. Simulation results demonstrate the effectiveness and feasibility of the proposed method.

Keywords

Underactuated capsule systems, trajectory planning, nonlinear geometric analysis, viscoelasticity

Introduction

The last two decades have witnessed a surge of contributions to the researches and applications of underactuated mechanical systems (UMSs). These systems are defined with fewer independent control inputs m than the degrees-of-freedom (DOF) n , and as such, $(n - m)$ degrees of freedom cannot be directly actuated and controlled. Synthesis of the control systems for UMSs, according to the Brockett's theorem (Brockett et al., 1983), is always challenging owing to the non-holonomic property, complicated internal dynamics and unavailability of feedback linearizability. As UMSs, the capsule systems (Fang and Xu, 2011; Huda and Yu, 2015; Kim et al., 2010; Liu et al., 2014, 2016; Yu, M. Nazmul Huda, et al., 2011) have become an increasingly active domain of research and received significant attentions. However, as recently reported in Shiriaev et al. (2014), it is always challenging to find an appropriate way to describe and characterize performance of the non-collocated subsystem owing to the underactuation and dynamic couplings.

The primary objectives of trajectory planning for autonomous capsule systems are optimal travel distance and fast average travel velocity. The internal force-static friction principle (Yamagata and Higuchi, 1995) has been well-employed (Bolotnik and Figurina, 2008; Fang and Xu, 2011; Huda et al., 2014; Kim et al., 2007; Lee et al., 2008; Liu, et al., 2013b; Liu et al., 2014; Wang et al., 2008; Yu et al., 2011). In

recent years, intensive researches have been conducted towards optimal periodic control modes of the internal driving mechanism, namely velocity-controlled mode (Lee et al., 2008; Li et al., 2006; Su et al., 2009; Yu et al., 2008) and acceleration-controlled mode (Fang and Xu, 2011; Yu et al., 2011). The minimal energy solution was obtained in Li et al. (2006) to generate a four-step motion pattern. An optimal controller was designed with experimental comparison in Lee et al. (2008). A four-step acceleration profile was proposed in Yu et al. (2011) for the motion control of capsubots. The stick-slip effect was considered and elaborately analysed by Fang and Xu (2011) to optimize the parameters of the internal controlled mass to obtain maximal average steady-state velocity. It is evident that friction plays pivotal roles in propulsion and locomotion for self-propelled capsule systems. In the fast motion stage, the system is propelled to move back and forth under the underactuated dynamics and nonlinear friction, which contributes to the net progressions. Therefore, describing and characterizing the coupling behaviour, which are

¹Faculty of Science and Technology, Bournemouth University, UK

²Faculty of Management, Bournemouth University, UK

Corresponding author:

Hongnian Yu, Faculty of Science and Technology, Bournemouth University, Poole BH12 5BB, UK.

Email: yuh@bournemouth.ac.uk

difficult and challenging, are of vital importance particularly for efficient trajectory planning. Unfortunately, a majority of reported results in the literature, such as Li et al. (2006) and Yu et al. (2008), were mainly devoted to the couplings in the slow motion stage, optimal control design of the fast motion was usually neglected. This is owing to the coupling dynamics that make the related analysis a difficult task. Towards trajectory construction, it is worth mentioning that there are several significant studies for overhead cranes systems based on phase plane analysis of crane kinematics (Sun et al., 2011, 2012), whilst as locomotion systems, the locomotion-performance indexes (e.g. average locomotion velocity, energy efficiency) were not examined. Indeed, it is a tough task to achieve steady-state periodic motion of the actuated subsystem and efficient system performance simultaneously.

In addition, it is well-established in control practices that smart actuators (e.g. piezoelectric actuators, shape memory alloys) may experience the lag problem (certain delay in time such as hysteresis) originated from magnetic, ferromagnetic and ferroelectric materials, which may occur between the application and the removal of a force (Hassani et al., 2014; Iyer et al., 2005; Wang and Su, 2006). It occurs with sudden changes in velocity/acceleration, and this is the circumstance of the capsule's motion. In order to drive the capsule body via coupling behaviour, the internal mechanism has to be actuated by the actuator with relatively higher velocity/acceleration. Besides, the nonlinear interaction between actuator and driving mechanism needs to be characterized such that practical engineering requirements can be met. In this paper, a novel trajectory planning approach for underactuated capsule locomotion is proposed. The nonlinear interaction between actuator and driving pendulum is characterized by a viscoelastic pair of torsional spring and viscous damper. The proposed method features geometric analysis of dynamic coupling, identification of optimal viscoelastic parameters and optimization of the trajectory parameters. The evaluation of the computational complexity of the proposed algorithm through real-time implementation will be conducted in due course. The main contributions of this paper are as follows: (i) Designing a characterization algorithm towards the underactuation-induced dynamic couplings using the nonlinear geometric analysis approach. (ii) Proposing kernel practical control indexes in the presence of viscoelastic property and the jag problem, and construct an analytical motion trajectory with promising efficacy and characteristics in continuity and smoothness, which facilitate the design of tracking controller. (iii) Developing an analytical parameterization algorithm for optimization of the trajectory parameters.

The paper is organized as follows. The capsule system and modelling are presented in the second section. The problem formulation is given in the third section. The trajectory planning algorithm is detailed in the fourth section with the design of a tracking controller. Simulation results are provided and discussed in the fifth section. Finally, conclusions are given in the sixth section.

The capsule system and modelling

Definition 1: The set of DOF of UMSs can be partitioned into two subsets (Spong, 1998), which referred to as

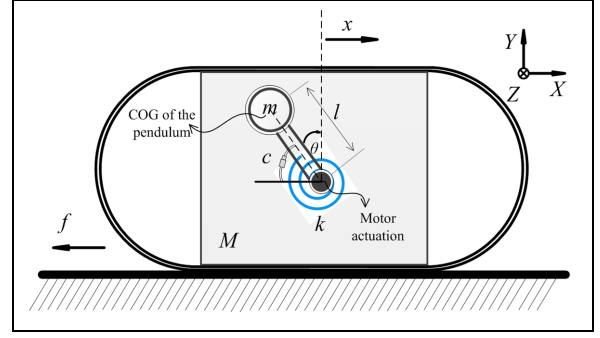


Figure 1. Schematic of the encapsulated system.

collocated subset with its cardinality contains the actuated DOF and equals the number of control inputs; and non-collocated subset accounts for the remaining non-actuated DOF.

The considered capsule system is shown in Figure 1, which contains a pendulum (with length l and mass m) and a platform (with mass M) merged with the rigid massless capsule shell. The actuator is mounted at the pivot to rotate the pendulum. The interaction between the actuator and the pendulum is described by a linear viscoelastic pair of torsional spring with elastic coefficient k and damper with viscous coefficient c . It is assumed that the mass of the pendulum is centralized at the ball and the center of mass of the platform coincides with the pivot axis. As a result, the capsule motion is constrained on XY plane. In what follows, for the sake of brevity, s_θ , c_θ and S_x will be employed to denote the trigonometric function $\sin\theta$, $\cos\theta$ and the signal function $\text{Sign}(\dot{x})$, respectively.

The capsule system works as follows. The capsule body is propelled over a surface rectilinearly via interaction between the driving force and the sliding friction, generating alternative sticking and slipping locomotion. Meanwhile, the elastic potential energy is stored and released alternatively in compatible with contraction and relaxation of the torsional spring. The motion of capsule starts with static state, and it moves when the magnitude of resultant force applied on its body in the horizontal direction exceeds the maximal value of the friction force. It is termed as the sticking phase when the above condition is not satisfied. At the instant the condition is met, the sticking phase is annihilated and the capsule body moves progressively, this fast motion is called the slipping phase. Therefore, friction is a vital factor for optimal control of the stick-slip locomotion.

The underactuated capsule dynamics are derived using the Euler-Lagrangian approach as

$$M(q)\ddot{q} + C(q, \dot{q})\dot{q} + K(q)q + G(q) + F_d = Bu \quad (1)$$

where $q(t) = [\theta x]^T$ represents the system state vector. $M(q) \in \mathcal{R}^{2 \times 2}$ is the inertia matrix, $C(q, \dot{q}) \in \mathcal{R}^{2 \times 2}$ denotes the Centripetal-Coriolis matrix, $K(q) \in \mathcal{R}^{2 \times 2}$ is the generalized stiffness matrix, $G(q) \in \mathcal{R}^{2 \times 1}$ represents the gravitational torques, $B \in \mathcal{R}^{2 \times 1}$ is the control input vector, $F_d(t)$ denotes the frictional torques, $u \in \mathcal{R}^1$ is the control input applied to

the system. Details of the variables above are listed as follows:

$$M(q) = \begin{bmatrix} ml^2 & -mlc_\theta \\ -mlc_\theta & (M+m) \end{bmatrix}, \quad C(q, \dot{q}) = \begin{bmatrix} 0 & 0 \\ mls_\theta \dot{\theta} & 0 \end{bmatrix},$$

$$K(q) = \begin{bmatrix} k & 0 \\ 0 & 0 \end{bmatrix}, \quad G(q) = [-mgl s_\theta 0]^T, \quad B = [10]^T \quad \text{and}$$

$F_d(t) = [c\dot{\theta}f]^T$. f denotes the sliding friction force. Note that, in this paper, the Coulomb friction model $f = \begin{cases} \mu(M + F_y)S_x, & \text{for } \dot{x} \neq 0 \\ f_0, & \text{for } \dot{x} = 0 \end{cases}$ is assumed, with

$F_y = mg - ml\dot{\theta}^2 c_\theta - ml\ddot{\theta} s_\theta - (k\theta + c\dot{\theta})s_\theta/l$ be the internal reaction forces applied on the pendulum by the platform in the vertical direction, f_0 denotes the stiction force when capsule speed is zero. μ and c represent the coefficient of sliding friction and the motor viscous friction at the pivot, respectively. $g \in \mathcal{R}^+$ is the gravitational acceleration. The capsule dynamics encompass the collocated and non-collocated subsystems, wherein the latter one contains the system kinematics that capture the coupling behaviours between the driving pendulum and the capsule body.

Remark 1: The contact interface is anisotropic, and asymmetry characteristic may arise owing to physical and structural inconsistency of the system parameters. It is plausible that the stiction force f_0 exists with its value falling into the threshold of the Coulomb friction, that is, $[-\mu(M + F_y)S_x, \mu(M + F_y)S_x]$. This is owing to the sticking motion and largely relying on the magnitudes of the external forces. In this paper, we assume that there is no friction force applied on the capsule when it keeps stationary ($\dot{x} = 0$). The studies on dynamic frictions will be reported in due course.

Harmonic excited forces have been employed to generate periodic motions for capsule systems as studied in Liu et al. (2013a, 2013b). On this occasion, forward and backward motions can be generated and controlled via proper tuning of the control parameters. Utilizing the harmonic force Ac_Ω with amplitude A and frequency Ω to excite the pendulum, and introducing the characteristic time scale $\omega_n = \sqrt{g/l}$ and the characteristic length $x_0 = g/\omega_n^2$ to obtain the non-dimensional equations of motion, we have

$$[\mathcal{M}]\{\ddot{\mathbf{h}}\} + [\mathcal{C}]\{\dot{\mathbf{h}}\} + [\mathcal{K}]\{\mathbf{h}\} + [\mathcal{G}] + [\mathcal{F}_d] = \{\mathcal{U}\}u_d \quad (2)$$

where $[\mathcal{M}] = \begin{bmatrix} 1 & -c_\theta \\ -c_\theta & \lambda + 1 \end{bmatrix}$, $[\mathcal{C}] = \begin{bmatrix} 0 & 0 \\ s_\theta \dot{\theta} & 0 \end{bmatrix}$, $[\mathcal{K}] = \begin{bmatrix} \rho & 0 \\ 0 & 0 \end{bmatrix}$, $[\mathcal{G}] = \begin{bmatrix} -s_\theta \\ 0 \end{bmatrix}$, $\{\mathcal{U}\} = \begin{bmatrix} 1 \\ 0 \end{bmatrix}$ and $[\mathcal{F}] = \begin{bmatrix} v\dot{\theta} \\ f' \end{bmatrix}$, $u_d = hc_{\omega\tau}$ and $f' = \mu[(\lambda + 1) - s_\theta \ddot{\theta} - c_\theta \dot{\theta}^2 - (\rho\theta + v\dot{\theta})s_\theta]S_x$.

The derivations above are conducted *w.r.t.* the dimensionless time $\tau = \omega_n t$ and the configuration variables are transformed to $\{\mathbf{h}\} = [\xi_1 \xi_2]^T = [\Theta X]^T$. The dot (\cdot) in (2) denotes the derivative in the scaled time coordinate. The rest of the non-dimensional quantities are defined as

$$X = x/x_0, \lambda = M/m, \rho = k/(ml^2\omega_n^2), v = c/(ml^2\omega_n),$$

$$h = A/(ml^2\omega_n^2), \omega = \Omega/\omega_n \quad (3)$$

Remark 2: Nondimensionalization of the governing equations can simplify the analysis of the model through searching the dimensionless groups that control its solution patterns. Under the dimensionless coordinate, the physical meanings of the control parameters are captured as: λ is the mass ratio, ρ and v respectively denote the normalized elastic and viscous coefficients, h and ω are the normalized excitation amplitude and frequency.

Problem formulation

A typical time history of the system performance after initial transients is presented in Figure 2, wherein the capsule displacement and pendulum angular velocity are shown. It is evident that the net capsule displacement during one cycle of excitation \mathbf{R} is mainly determined by the ramp edges of the harmonic force in forward motion stage \mathbf{R}_F . However, such periodic motions are essentially not optimal, since for each motion cycle, the forward displacement obtained in \mathbf{R}_F is partly counteracted in the forthcoming backward motion stage \mathbf{R}_B , and excessive energy are consumed owing to the backward journey.

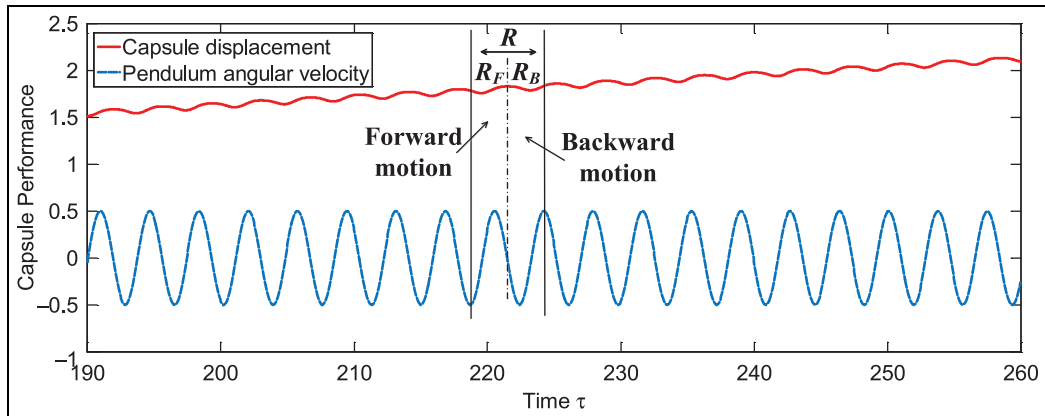


Figure 2. Time histories of typical steady-state capsule motion.

Therefore, a two-stage motion trajectory needs to be constructed that optimally utilizes the ramp edges of the harmonic excitation in the forward motion stage and thereafter, sufficiently neutralize the backward motions via optimal control of the sticking phase and friction. The definitions are given as follows:

Definition 2: Progressive stage: driving the pendulum with higher angular acceleration incorporating with the release of the elastic energy stored in the torsional spring that leads the capsule to overcome the maximal static friction to generate a slipping motion ($\dot{X} \neq 0$).

Definition 3: Restoring stage: returning the pendulum to initial position slowly to restore the potential energy and prepare for the next cycle, the resultant force exerting on the capsule body in horizontal direction is less than the maximum dry friction, that is, the capsule is kept in the sticking phase in this stage ($\dot{X} = 0$).

Based on the practical control indexes and dynamic constraints associated with the stick-slip locomotion of the capsule, the following principles are designed as objectives need to be achieved to construct an optimal motion trajectory for the driving pendulum:

Principle 1: For each motion cycle, the pendulum is constrained rotating within an advisable angle range, indicating that the upper and lower boundaries are given as

$$|\Theta(\tau)| \leq \Theta_0 \quad (4)$$

where Θ_0 is the prescribed angular displacement of the driving pendulum.

Principle 2: The angular velocity and angular acceleration of the driving pendulum need to be placed within bounded ranges, given by

$$|\dot{\Theta}(\tau)| \leq v_\Theta, |\ddot{\Theta}(\tau)| \leq a_\Theta \quad (5)$$

where $v_\Theta \in \mathbb{R}^+$ and $a_\Theta \in \mathbb{R}^+$ are absolute boundary values of the angular velocity and acceleration, respectively.

Principle 3: The capsule is contacting with the sliding surface, in order to achieve a non-bounding motion, a constraint for the contact force needs to be satisfied, which means the contact force has to be always greater than zero, gives

$$(\lambda + 1) - s_\Theta \ddot{\Theta} - c_\Theta \dot{\Theta}^2 - (\rho\Theta + v\dot{\Theta})s_\Theta > 0 \quad (6)$$

Principle 4: The capsule has to be remained stationary after one cycle of forward motion to wait for the pendulum's return. In this occasion, the force of the driving pendulum applied on the capsule in horizontal direction has to be less than the maximal static friction, gives

$$\begin{aligned} &|c_\Theta \ddot{\Theta} - s_\Theta \dot{\Theta}^2 + (\rho\Theta + v\dot{\Theta})c_\Theta| \leq \mu \\ &[(\lambda + 1) - s_\Theta \ddot{\Theta} - c_\Theta \dot{\Theta}^2 - (\rho\Theta + v\dot{\Theta})s_\Theta] \end{aligned} \quad (7)$$

Remark 3: Principles 1 and 2 are associated with the collocated subsystem, which is prone to control and convenient to

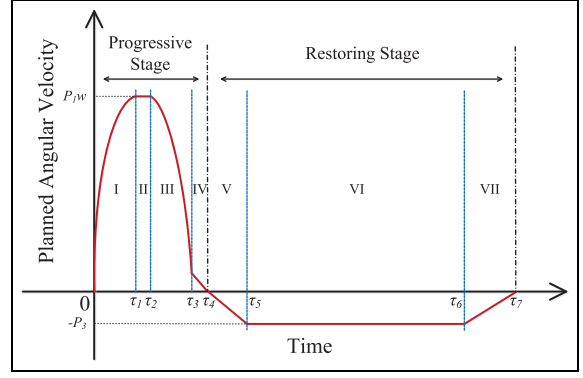


Figure 3. Schematic profile for the synchronized velocity trajectory.

achieve, whilst Principles 3 and 4 are of vital importance for the non-collocated capsule locomotion and energy efficacy. Therefore, as one major contribution, both of these principles are explicitly considered through the nonlinear geometric analysis method.

In addition, a transition function (Phase II as shown in Figure 3) is introduced to cope with the jag problem and to synchronize the motion trajectory. Figure 3 depicts the proposed two-stage velocity trajectory based on the aforementioned control indexes, objectives and synchronization considerations. The planned trajectory is described as

$$\dot{\Theta}(\tau) = \begin{cases} P_1\omega s_{\omega\tau}, \tau \in [0, \tau_1) \\ P_1\omega, \tau \in [\tau_1, \tau_2) \\ P_1\omega s_{\omega\tau - \tau_2}, \tau \in [\tau_2, \tau_3) \\ \frac{\tau_3 - \tau}{\tau_3 - \tau_2} P_2, \tau \in [\tau_3, \tau_4) \\ \frac{\tau_3 - \tau}{\tau_4 - \tau_3} P_3, \tau \in [\tau_4, \tau_5) \\ -P_3, \tau \in [\tau_5, \tau_6) \\ \frac{\tau_6 - \tau}{\tau_5 - \tau_6} P_3, \tau \in [\tau_6, \tau_7) \end{cases} \quad (8)$$

where $P_1\omega$ and P_3 are upper and lower trajectory boundaries, respectively. P_2 is the critical boundary when the capsule keeps stationary, ω is the frequency of excitation.

Geometric analysis-based trajectory planning

Definition 4: Poincaré maps: one considers a periodic orbit with initial conditions within a section of the space, samples the solution of a system according to an event-based or time-based rule, and then evaluates the stability properties of equilibrium points (or fixed points) of the sampled system (Westervelt et al., 2007).

It is evident from (6) and (7) that Principles 3 and 4 are susceptible to the elastic coefficient ρ and viscous coefficient v , which are vital factors for energy consumption. In this section, a novel approach is explored to characterize the

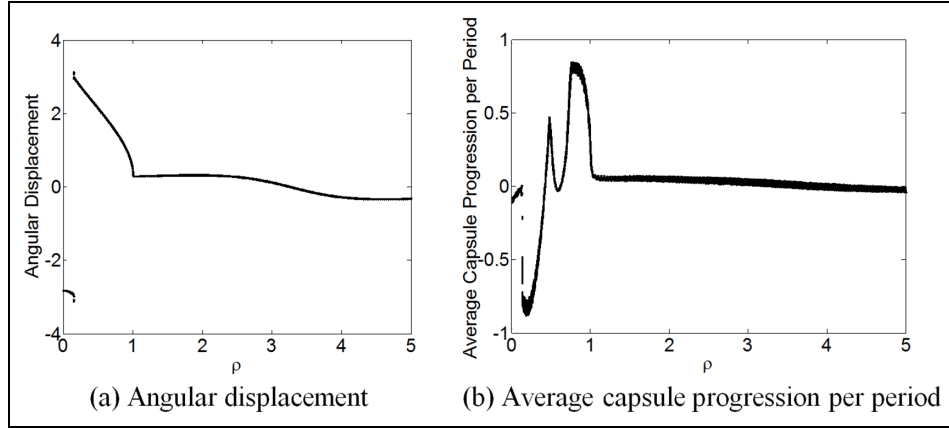


Figure 4. Qualitative variation laws of ρ obtained for $h = 0.8$, $\omega = 1.7$, $\nu = 0.8$ and $\lambda = 3.6$.

(a) Angular displacement; (b) Average capsule progression per period.

coupling and identify the qualitative variation laws in terms of the capsule performance, such that the optimal viscoelastic parameters are selected beforehand and fed into parameterization of the motion trajectory. Concretely, when the control indexes and non-collocated dynamic constraints are considered, the proposed geometric analysis-based trajectory planning algorithm is given by:

Algorithm 1: Construction and optimization of motion trajectory.

Step 1. Compute and project the underactuated dynamics onto the dimensionless Poincaré maps;

Step 2. Describe and characterize coupling between the collocated and non-collocated subsystems, and identify the optimal viscoelastic parameters via capsule locomotion-performance index;

Step 3. Characterize the dynamic constraints for stick-slip progression through rigorous analytical analysis towards underactuation and internal coupling;

Step 4. Compute the trajectory boundaries;

Step 5. Optimize and parameterize the planned trajectory for each phase with identified optimal viscoelastic parameters from Step 2, characterized the conditions for optimal stick-slip progression from Step 3 and computed trajectory boundaries from Step 4.

Remark 4: Poincaré maps are able to sample the solution of a system according to an event-based or time-based rule, and then evaluate the stability properties of equilibrium points (or fixed points) of the sampled system. The proposed algorithm utilizes the knowledge from both collocated and non-collocated subsystems to facilitate efficient locomotion of the capsule system. The computation and projection of dynamics onto an induced hyper-manifold of the closed-loop system enables convenient analysis and characterization of the underactuated couplings.

Coupling characterization and viscoelastic parameter identification

In this subsection, coupling behaviour and qualitative variation laws induced by the viscoelastic parameters for the progressive stage are firstly characterized and identified. From the viewpoint of energy, it is evident that efficient utilizations of potential energy stored in the spring and dissipative energy in the damper are crucial factors for energy efficacy. The average progression per period is characterized geometrically to examine the locomotion-performance index.

Qualitative variation law of the elastic coefficient ρ is presented in Figure 4. The effects of ρ on the pendulum and capsule subsystems are shown in Figures 4(a) and 4(b), respectively. It is also observed in Figure 4(a) that a grazing of angular displacement occurs at $\rho = 0.25$, and thereafter the angular displacement largely decreases as ρ increases. As a locomotion system, the average locomotion speed is of vital importance for locomotion system, in this regard, the average capsule progression per period of excitation is characterized and shown in Figure 4(b), wherein the global maximum and minimum average progression points are recorded at $\rho = 0.9$ and $\rho = 0.25$, respectively. A pair of locally maximal and minimal points of average progressions is also identified at $\rho = 0.65$ and $\rho = 0.75$. Time histories of the capsule displacements for $\tau \in [370, 400]$ are presented in Figure 5 to verify the identified variation law. It indicates that for a smaller coefficient at $\rho = 0.1$, the spring is insufficient to generate enough force to enhance the capsule progression, accordingly the capsule performs vibrational motion around the starting point. Similarly, for a larger coefficient at $\rho = 2.0$, the spring becomes sufficiently 'hard' to trap the capsule progression. For the values in between, the spring either contributes to the forward motions of the capsule (e.g. $\rho = 0.7, 0.9$), or drags it backwards in the opposite direction (e.g. $\rho = 0.3, 0.25$).

Figure 6 presents the qualitative variation law of viscous coefficient ν . From Figure 6(a), it is observed that as ν increases, the angular displacement decreases monotonously.

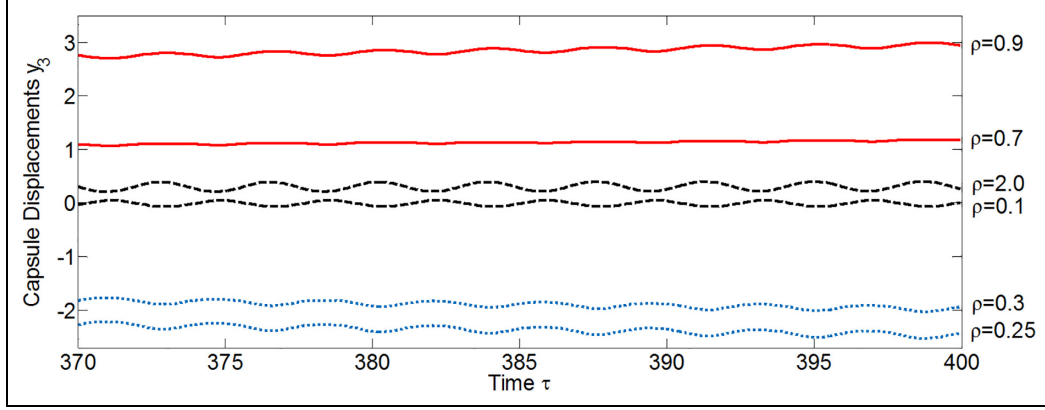


Figure 5. Time histories of the capsule displacements.

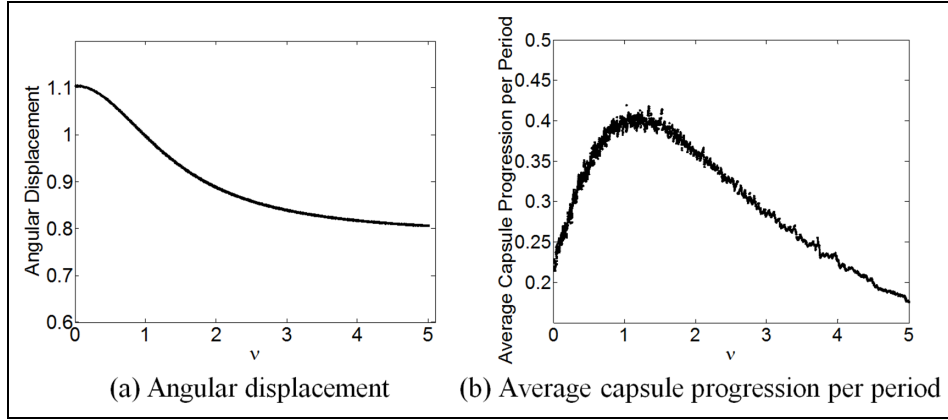


Figure 6. Qualitative variation laws of ν obtained for $h = 0.8$, $\omega = 1.7$, $\rho = 0.9$ and $\lambda = 3.6$.
(a) Angular displacement; (b) Average capsule progression per period.

However, it seems insufficient to identify and conclude the effects of ν on the capsule performance through the observation on the pendulum subsystem. Therefore, the average capsule progression per period of excitation is portrayed in Figure 6(b), where the maximum average progression point is recorded at $\nu = 1.3$. Interestingly, from Figure 6(b) it is noted that the capsule progression increases monotonically as ν augments for $\nu \in (0, 1.3]$; on the other hand, the viscosity acts negative roles by decreasing the capsule's forward progression for $\nu \in (1.3, 5.0]$. The identified optimal viscous value is critical for the system and controller design. Time histories of the capsule displacements for $\tau \in [370, 400]$ are presented in Figure 7 to verify the qualitative variation law.

Remark 5: As shown in Figures 4(a) and 6(a), the performance of the collocated subsystem can be conveniently evaluated using conventional approaches via the affined projection, whilst it is a challenging task to evaluate the non-collocated subsystem. The proposed approach can characterize the internal dynamic couplings such that the non-collocated capsule performance is evaluated beforehand through the locomotion-performance index. The optimal values of viscoelastic parameters can be identified accordingly.

From Figures 5 and 7, it is obvious that the backward motions decrease the locomotion efficacy. To sufficiently suppress the effect of backward motions, the sticking phase needs to be controlled at the restoring stage through dynamic interactions with the sliding friction, which will be discussed in the following subsections.

Dynamic constraints characterization

Conventional motion planning approaches are not directly applicable to the capsule subsystem that is non-collocated; as such, the dynamic constraints (6) and (7) imposed on the capsule locomotion need to be fully considered when planning an efficient nominal forced trajectory. The following propositions are given to characterize the constrained stick-slip motions.

Proposition 1: From Principle 3, the non-bounding motion for the capsule can be achieved if the following condition is satisfied

$$\dot{\theta}^2 |(\theta + \rho\theta + \nu\dot{\theta})| < \varpi^2/2 \quad (9)$$

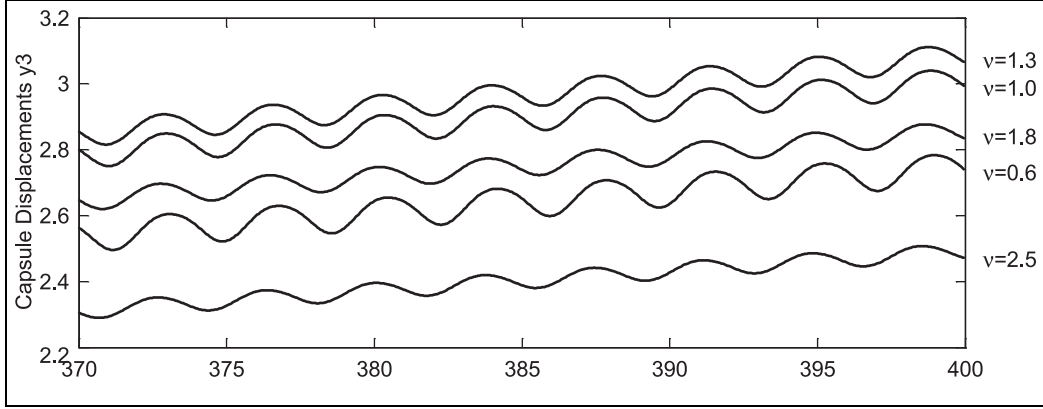


Figure 7. Time histories of the capsule displacements.

where

$$\varpi = \lambda + 1$$

Proof: From Principle 3, we have

$$(\theta^+ \rho \theta + v \dot{\theta})_{s_\theta} + \dot{\theta}^2 c_\theta < (\lambda + 1) \quad (10)$$

Using the auxiliary angle formula and enlarging the inequality, a sufficient condition is given as

$$\sqrt{(\theta^+ \rho \theta + v \dot{\theta})^2 + \dot{\theta}^4} < (\lambda + 1) \quad (11)$$

Then employing the AM-GM inequality theorem yields

$$\sqrt{2\dot{\theta}^2(\theta^+ \rho \theta + v \dot{\theta})} < (\lambda + 1) \quad (12)$$

Therefore, we have

$$\dot{\theta}^2 |(\theta^+ \rho \theta + v \dot{\theta})| < (\lambda + 1)^2 / 2 \quad (13)$$

Proposition 2: From Principle 4, the sticking motion for the platform in the restoring stage can be achieved if the following condition is satisfied

$$\theta^+ \dot{\theta}^2 + \rho \theta + v \dot{\theta} \leq \varpi \vartheta \quad (14)$$

where

$$\varpi = \lambda + 1, \vartheta = \mu / \sqrt{\mu^2 + 1}$$

Proof: Utilizing the forces in the horizontal and vertical directions, removing the absolute value sign and considering one side of the inequality that

$$c_\theta \bar{\theta} s_\theta \dot{\theta}^2 + (\rho \theta + v \dot{\theta}) c_\theta \leq \mu \left[(\lambda + 1) - s_\theta \bar{\theta} c_\theta \dot{\theta}^2 - (\rho \theta + v \dot{\theta}) s_\theta \right] \quad (15)$$

Reorganizing (15), we have

$$(\mu s_\theta \theta^+ c_\theta \dot{\theta}) + (\mu c_\theta \dot{\theta}^2 - s_\theta \dot{\theta}^2) + [\mu(\rho \theta + v \dot{\theta}) s_\theta + (\rho \theta + v \dot{\theta}) c_\theta] \leq \mu(\lambda + 1) \quad (16)$$

Using the auxiliary angle formula and enlarging the inequality, a sufficient condition is given as

$$\sqrt{\mu^2 + 1} (\theta^+ \dot{\theta}^2 + \rho \theta + v \dot{\theta}) \leq \mu(\lambda + 1) \quad (17)$$

Therefore, we have

$$\theta^+ \dot{\theta}^2 + \rho \theta + v \dot{\theta} \leq \mu(\lambda + 1) / \sqrt{\mu^2 + 1} \quad (18)$$

Trajectory boundaries computation

The aim of optimization is to maximize the average capsule speed during one motion cycle through appropriate design of the velocity trajectory profile. Thus, a series of parameters need to be selected, including the durations for each phase $\tau_1 \sim \tau_7$ and trajectory boundaries P_1 , P_2 and P_3 . Based on the constraints characterized above, the boundary conditions are defined as

$$\begin{aligned} \theta(\tau_0) = \theta(\tau_7) = -\theta_0 < 0, \theta(\tau_3) = \theta_0, \dot{\theta}(\tau_0) = 0, \dot{\theta}(\tau_0) \\ = \dot{\theta}(\tau_3) = \dot{\theta}(\tau_7) = 0 \end{aligned}$$

Considering the planned trajectory (8) in the duration $[0, \tau_3]$, P_2 can be explicitly obtained through integral calculation of the system dynamics (2) under the consideration of θ_0 that if $c_{\theta_0} + \mu s_{\theta_0} \neq 0$. Therefore, we have

$$P_2 = \dot{\theta}(\tau_3) = \left[\mu(\lambda + 1)\tau_3 - \mu\rho \int_0^{\tau_3} \theta s_\theta d\tau + \mu v \left(\theta s_\theta - \int_0^{\tau_3} \theta c_\theta d\tau \right) \right] / (c_{\theta_0} + \mu s_{\theta_0}) \quad (19)$$

In addition, utilizing the principle of energy conservation in Figure 3, the following formulations can be obtained as

$$\int_0^{\tau_1} P_1 \omega s_{\omega\tau} d\tau + P_1 \omega (\tau_2 - \tau_1) + \int_{\tau_2}^{\tau_3} P_1 \omega s_{\omega_1 \tau - \tau_2} d\tau - \frac{1}{2} P_2 \left[\frac{N\pi}{\omega_1} + \tau_2 - \tau_3 \right] = 2\Theta_0 \quad (20)$$

$$\frac{1}{2}(-P_3)[(\tau_7 - \tau_4) + (\tau_6 - \tau_5)] = \frac{1}{2}P_2(\tau_4 - \tau_3) + 2\Theta_0 \quad (21)$$

Therefore, the lower and critical trajectory boundaries are obtained as

$$P_2 = \{2P_1[1 - c_{\omega\tau_1} + \omega(\tau_2 - \tau_1) + c_{\omega\tau_2} - c_{\omega\tau_3 - \tau_2}] - 4\Theta_0\} / (N\pi/\omega_1 + \tau_2 - \tau_3) \quad (22)$$

$$P_3 = [4\Theta_0 + P_2(\tau_4 - \tau_3)] / (\tau_7 - \tau_4) + (\tau_6 - \tau_5) \quad (23)$$

Trajectory parameterization

Theorem 1: Consider the capsule system (2) and the planned trajectory (8) with dynamic constraints (4)-(7) and the viscoelastic property, if the trajectory parameters are chosen as

$$\begin{aligned} \tau_1 &= \left(\frac{\varpi^2}{2(P_1\omega)^3} - v \right) / \rho, \tau_2 = \omega\tau_3 - \arcsin \frac{P_2}{P_1\omega}, \tau_3 = \frac{N\pi}{\omega}, \\ \tau_4 &= -\frac{P_2}{\varpi\vartheta - P_2^2 - \rho P_2\tau_3 - vP_2} + \tau_3, \\ \tau_5 &= \frac{\varpi\vartheta - P_3^2 - vP_3}{\rho P_3}, \tau_6 = \frac{[4\Theta_0 + \tau_4(P_2 + 2P_3) - P_2\tau_3]}{2P_3} \\ \text{and } \tau_7 &= (4\Theta_0 - P_2\tau_3 + P_2\tau_4 + 2P_3\tau_5) / 2P_3 \end{aligned} \quad (24)$$

Then the following properties hold:

- 1) the planned trajectory (8) is analytical;
- 2) Principles 1–4 are satisfied;
- 3) the time per period of locomotion can be evaluated beforehand as $T_{total} = \sum_{i=1}^7 \tau_i$.

Proof: To optimally parameterize the motion trajectory, the dynamic constraints are explicitly utilized with the identified optimal viscoelastic parameters ρ and v . Specifically, for Phase I, from Proposition 1, we have

$$\dot{\Theta}^2(\tau_1) \left| \left(\dot{\Theta} + \rho\Theta(\tau_1) + v\dot{\Theta}(\tau_1) \right) \right| < \varpi^2/2 \quad (25)$$

where $\dot{\Theta}(\tau_1) = P_1\omega$, $\ddot{\Theta}(\tau_1) = 0$ and $\Theta(\tau_1) = P_1\omega\tau_1$. The upper boundary of Phase I is obtained as

$$\tau_1 = \left(\frac{\varpi^2}{2(P_1\omega)^3} - v \right) / \rho \quad (26)$$

The formulation for Phase II can be described as $P_1\omega s_{\omega\tau_3 - \tau_2} = P_2$, accordingly its duration can be derived as

$$\tau_2 = \omega\tau_3 - \arcsin P_2/P_1\omega \quad (27)$$

In view of the synchronization consideration, the motion trajectory is designed to reach the amplitude of the harmonic excitation at time τ_1 and keep it until time τ_2 , and duration of this phase has to be half of the excitation period, which gives the duration Phase III as

$$\tau_3 = N\pi/\omega \quad (28)$$

During Phase IV, the capsule is kept stationary that allows a recovery process without any backward motion. Applying Proposition 2 at time τ_3 , gives

$$\ddot{\Theta}(\tau_3) + \dot{\Theta}(\tau_3)^2 + \rho\Theta(\tau_3) + v\dot{\Theta}(\tau_3) \leq \varpi\vartheta \quad (29)$$

where $\Theta(\tau_3) = P_2\tau_3$, $\dot{\Theta}(\tau_3) = P_2$ and $\ddot{\Theta}(\tau_3) = -P_2/(\tau_4 - \tau_3)$. Then the duration τ_4 can be obtained as

$$\tau_4 = -P_2/(\varpi\vartheta - P_2^2 - \rho P_2\tau_3 - vP_2) + \tau_3 \quad (30)$$

In terms of Phase V, applying Proposition 2 at time τ_5 , we have

$$\ddot{\Theta}(\tau_5) + \dot{\Theta}(\tau_5)^2 + \rho\Theta(\tau_5) + v\dot{\Theta}(\tau_5) \leq \varpi\vartheta \quad (31)$$

where $\ddot{\Theta}(\tau_5) = 0$, $\dot{\Theta}(\tau_5) = P_3$, $\Theta(\tau_5) = P_3\tau_5$.

Accordingly, the maximal boundary of Phase V is calculated as

$$\tau_5 = (\varpi\vartheta - P_3^2 - vP_3) / \rho P_3 \quad (32)$$

Further relationship can be achieved in the duration of $[\tau_4, \tau_5]$ as

$$P_2(\tau_5 - \tau_4) = P_3(\tau_4 - \tau_3) \quad (33)$$

To determine the trajectory profile for Phase VI and Phase VII, it is noted that the durations of $[\tau_4, \tau_5]$ and $[\tau_6, \tau_7]$ are accordant based on the design objectives, gives

$$\tau_5 - \tau_4 = \tau_7 - \tau_6 \quad (34)$$

Combining (33) with (22), we have

$$\tau_6 = [4\Theta_0 + \tau_4(P_2 + 2P_3) - P_2\tau_3] / 2P_3 \quad (35)$$

$$\tau_7 = (4\Theta_0 - P_2\tau_3 + P_2\tau_4 + 2P_3\tau_5) / 2P_3 \quad (36)$$

The trajectory parameterization procedure (25)–(36) directly indicates the analytical property of the planned trajectory (8) and satisfaction of Principles (1) and (2). Propositions 1 and 2 ensure the satisfaction of Principles (3) and (4). Property (3) can be directly shown by adding the trajectory durations from (26), (27), (28), (30), (32), (35) and (36), that is, $T_{total} = \sum_{i=1}^7 \tau_i$.

Remark 6: It is noted that the trajectory planning scheme proposed in this work can be adopted either in the open-loop control system design or as feedforward segment in the

closed-loop control system formulation of the capsule systems. Admittedly, it is nearly impossible to implement trajectory planning algorithm merely in an open-loop control system to cope with the unexpected uncertainties (e.g. unstructured and unmodelled dynamics, external disturbances). Indeed, the proposed approach may be combined with advanced control schemes (e.g., robust and adaptive paradigms) to enhance robustness to disturbances and adaptability to parametric uncertainties with guaranteed performance of the proposed algorithm. The main concentration of this work is optimized trajectory planning for underactuated capsule systems; further considerations in advanced control are beyond the scope here and will be reported in another paper.

Remark 7: Indeed, evaluation of the computational complexity of the proposed algorithm through real-time implementation is of vital importance. While the main focus of the proposed work is to develop a novel off-line trajectory planning algorithm to make steps forward based on the previous researches. The motivation behind is that the analysis for dynamic coupling behaviour of the underactuated systems, which is of much difficulty and challenge, is the foundation to propose an appropriate trajectory. And few results have been reported on the off-line trajectory planning incorporating the dynamic coupling behaviour and viscoelastic property. Therefore, real-time implementation and evaluation of the computational complexity of the proposed algorithm are beyond the scope of the proposed work here and will be reported in due course.

Tracking controller design

To verify the capsule performance under the proposed trajectory planning scheme and to make convenient comparisons with the conventional approach, a tracking control system is designed in this subsection. Using the dynamic model in (2), we have

$$\left(1 - \frac{1}{\lambda + 1} c_\theta^2\right) \ddot{\theta} + \frac{1}{\lambda + 1} [c_\theta (s_\theta \dot{\theta}^2 + f')] - s_\theta + \rho\theta + v\dot{\theta} = u_d \quad (37)$$

Define the trajectory tracking error and its derivatives as

$$\tilde{\theta} = \theta - \theta_d, \quad \dot{\tilde{\theta}} = \dot{\theta} - \dot{\theta}_d \text{ and } \ddot{\tilde{\theta}} = \ddot{\theta} - \ddot{\theta}_d \quad (38)$$

Remark 7: It is noted that the duration of each motion phase is fixed, using equations of motion (2) and the planned trajectory, the prior knowledge of desired capsule and pendulum trajectories for each sampling time can be obtained by convenient computation.

Substituting (38) into (37) and conducting appropriate mathematical manipulation, we have the following system dynamics

$$\left(1 - \frac{1}{\lambda + 1} c_\theta^2\right) \ddot{\tilde{\theta}} = u_d - \frac{1}{\lambda + 1} [c_\theta (s_\theta \dot{\theta}^2 + f')] + s_\theta - \rho\theta - v\dot{\theta} - \left(1 - \frac{1}{\lambda + 1} c_\theta^2\right) \ddot{\theta}_d \quad (39)$$

Utilizing the collocated partial feedback linearization technique (Spong, 1998) for the system dynamics in (39), a feedback linearizing controller can be designed as

$$u_d = \left(1 - \frac{1}{\lambda + 1} c_\theta^2\right) \ddot{\theta}_d + \frac{1}{\lambda + 1} [c_\theta (s_\theta \dot{\theta}^2 + f')] - s_\theta + \rho\theta + v\dot{\theta} - K_v \left(1 - \frac{1}{\lambda + 1} c_\theta^2\right) \dot{\tilde{\theta}} - K_p \left(1 - \frac{1}{\lambda + 1} c_\theta^2\right) \tilde{\theta} \quad (40)$$

where K_v and K_p are positive control gains selected by the designer.

Substituting the tracking controller (40) into system (39), the closed-loop system can be obtained in the following form

$$\ddot{\tilde{\theta}} + K_v \dot{\tilde{\theta}} + K_p \tilde{\theta} = 0 \quad (41)$$

Therefore, it is evident through the Routh-Hurwitz criterion that the system stability is guaranteed, concretely, the designed tracking controller (40) drives the pendulum to follow the planned trajectory exponentially fast.

Simulation results

This section provides simulation results to verify the performance and effectiveness of the proposed scheme. Comparisons are made with Liu et al. (2014) (referred to as EPC system), in which a two-stage velocity trajectory is proposed using conventional approach with heuristically chosen control parameters. The parameters are allocated in original dimensions to make convenient comparisons. The system parameters are configured as $M = 0.5\text{kg}$, $m = 0.138\text{kg}$, $l = 0.3\text{m}$, $g = 9.81\text{m/s}^2$, $\mu = 0.01\text{N/ms}$ and system natural frequency $\omega_n = 5.7184\text{rad/s}$. Then, based on the proposed algorithms, the viscoelastic parameters are selected as $k = 0.36\text{Nm/rad}$ and $c = 0.0923\text{kgm}^2/\text{srad}$. The initial conditions are set as $\theta(0) = \theta_0 = \pi/3$, $\dot{\theta}(0) = 0$, $x(0) = 0$ and $\dot{x}(0) = 0$.

Step 1. Based on the trajectory planning algorithm presented in subsections 4.2–4.4, the optimal durations for each phase are calculated and detailed in Table 1, and therefore adopted to construct the optimal motion trajectory $\dot{\theta}_d$.

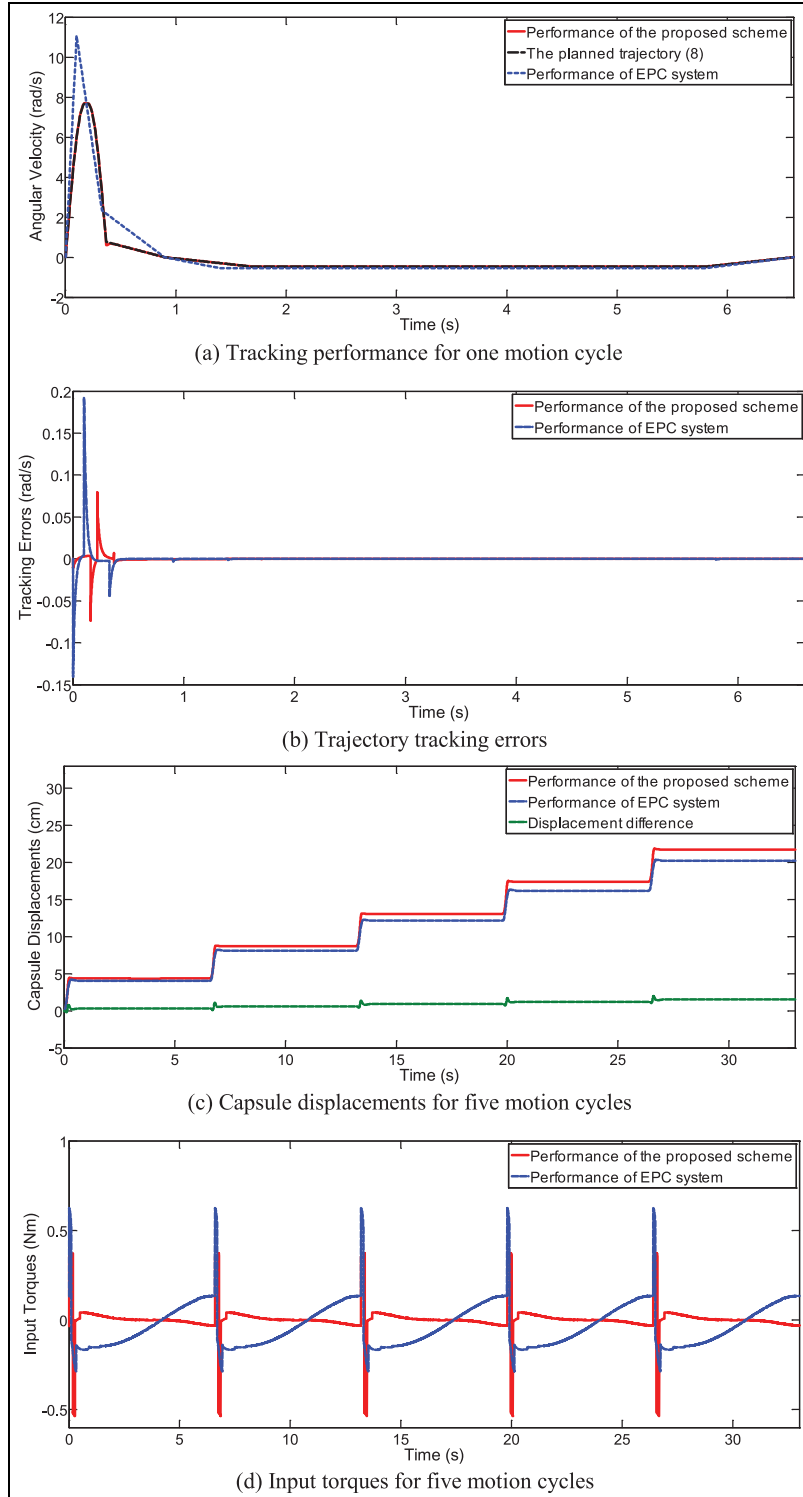
Step 2. To make convenient and rigorous comparisons, tracking control scheme (40) is employed for both capsule systems. The control gains are tuned and selected to achieve better control performance with values $K_v = 100$ and $K_p = 50$.

The simulation results are presented in Figure 8. It is observed that the driving pendulum tracks the planned trajectory accurately, and the maximum angular displacement, velocity and acceleration are bounded under physical constraints during each motion cycle. The trajectory tracking performances are presented in Figure 8(a). It is observed that the maximum angular velocity using the proposed approach is about 7.8 rad/s, which is lower than the EPC system with 11

AQ2

Table 1. Trajectory parameters for the simulation.

Trajectories	t_1	t_2	t_3	t_4	t_5	t_6	t_7
Trajectory EPC	0.1s	0.33s	0.9s	1.4s	5.8s	6.6s	NA
Trajectory (8)	0.133s	0.195s	0.275s	0.9s	1.7s	5.8s	6.6s

**Figure 8.** Performance of the capsule systems.

(a) Tracking performance for one motion cycle. (b) Trajectory tracking errors. (c) Capsule displacements for five motion cycles. (d) Input torques for five motion cycles.

rad/s. The trajectory tracking errors using the proposed method and the method for EPC system are shown in Figure 8(b), in which the proposed approach demonstrates better convergence of the tracking error. The synchronized trajectory also presents better transient performance in terms of the overshoot, and the absolute value of maximum pendulum swing is about 68.75° (17.1° smaller than the EPC system). These results have good agreements with the trajectory planning indexes and principles. The average velocity with the proposed trajectory calculated from Figure 8(b) for the first five cycles is 0.642cm/s, whereas it is 0.629cm/s for the EPC system. The distance-optimal property of the proposed approach is verified. The transition functions inserted into progressive stage guarantee the smooth transition, and thereafter a lower maximum input torque as shown in Figure 8(c) (0.5367 Nm compared with 0.6246 Nm of EPC system). This directly evidences a superior performance in terms of energy efficacy. The backward motions are sufficiently suppressed as can be seen from Figure 8(b). The results conclude that the stick-slip motions are efficiently controlled through the proposed method and therefore superior performance are guaranteed.

AQ3

Conclusions

In this paper, a novel geometric analysis-based trajectory planning scheme has been proposed for underactuated capsule systems with viscoelastic property. The non-collocated dynamic constraints have been considered into the control indexes, wherein it was found that characterization of the viscoelastic interaction plays a vital role in optimal control of the stick-slip motions with improved energy efficacy. The dynamic couplings have been characterized through rigorous geometric analysis on the Poincaré maps. The two-stage analytical motion trajectory has been constructed based on the control indexes and dynamic constraints, which have been evaluated analytically. The trajectory has been optimized and parameterized via rigorous analysis. A tracking controller has been designed to make the pendulum track the planned trajectory. The effectiveness and efficacy of the proposed approach have been verified through simulation studies. Future work will be emphasized on real-time implementation, advanced control schemes and experimental studies.

Declaration of conflicting interest

The authors declare that there is no conflict of interest.

Funding

This research received no specific grant from any funding agency in the public, commercial or not-for-profit sectors.

References

- Bolotnik NN and Figurina TY (2008) Optimal control of the rectilinear motion of a rigid body on a rough plane by means of the motion of two internal masses. *Journal of Applied Mathematics and Mechanics* 72(2): 126–135.
- Brockett RW and others (1983) Asymptotic stability and feedback stabilization. *Differential geometric control theory* 27(1): 181–191.

AQ4

- Fang H and Xu J (2011) Dynamics of a mobile system with an internal acceleration-controlled mass in a resistive medium. *Journal of Sound and Vibration* 330(16): 4002–4018.
- Hassani V, Tjahjowidodo T and Do TN (2014) A survey on hysteresis modeling, identification and control. *Mechanical Systems and Signal Processing* 49(1–2): 209–233.
- Huda MN and Yu H (2015) Trajectory tracking control of an underactuated capsbot. *Autonomous Robots* 39(2): 183–198.
- Huda MN, Yu H and Cang S (2014) Behaviour-based control approach for the trajectory tracking of an underactuated planar capsule robot. *IET Control Theory & Applications* 9(2): 163–175.
- Iyer RV, Tan X and Krishnaprasad PS (2005) Approximate inversion of the Preisach hysteresis operator with application to control of smart actuators. *IEEE Transactions on Automatic Control* 50(6): 798–810.
- Kim HM, Yang S, Kim J, et al. (2010) Active locomotion of a paddling-based capsule endoscope in an in vitro and in vivo experiment (with videos). *Gastrointestinal Endoscopy* 72(2): 381–387.
- Kim J-S, Sung I-H, Kim Y-T, et al. (2007) Analytical model development for the prediction of the frictional resistance of a capsule endoscope inside an intestine. *Proceedings of the Institution of Mechanical Engineers, Part H: Journal of Engineering in Medicine* 221(8): 837–845.
- Lee N, Kamamichi N, Li H, et al. (2008) Control system design and experimental verification of Capsbot. In: *IEEE/RSJ International Conference on Intelligent Robots and Systems, 2008. IROS 2008*, pp. 1927–1932.
- Li H, Furuta K and Chernousko FL (2006) Motion generation of the capsbot using internal force and static friction. In: *2006 45th IEEE Conference on Decision and Control*, pp. 6575–6580.
- Liu P, Yu H and Cang S (2014) Modelling and control of an elastically joint-actuated cart-pole underactuated system. In: *2014 20th International Conference on Automation and Computing (ICAC)*, pp. 26–31. IEEE.
- Liu P, Yu H and Cang S (2016) Modelling and dynamic analysis of underactuated capsule systems with friction-induced hysteresis. In: *2016 IEEE/RSJ International Conference on Intelligent Robots and Systems (IROS)*, pp. 549–554. IEEE.
- Liu Y, Pavlovskaja E, Hendry D, et al. (2013a) Vibro-impact responses of capsule system with various friction models. *International Journal of Mechanical Sciences* 72: 39–54.
- Liu Y, Wiercigroch M, Pavlovskaja E, et al. (2013b) Modelling of a vibro-impact capsule system. *International Journal of Mechanical Sciences* 66: 2–11.
- Shiriaev AS, Freidovich LB and Spong MW (2014) Controlled invariants and trajectory planning for underactuated mechanical systems. *IEEE Transactions on Automatic Control* 59(9): 2555–2561.
- Spong MW (1998) Underactuated mechanical systems. In: *Control Problems in Robotics and Automation*. Springer, pp. 135–150.
- Su G, Zhang C, Tan R, et al. (2009) A linear driving mechanism applied to capsule robots. In: *2009 International Conference on Networking, Sensing and Control*, pp. 206–209.
- Sun N, Fang Y, Zhang X, et al. (2011) Phase plane analysis based motion planning for underactuated overhead cranes. In: *2011 IEEE International Conference on Robotics and Automation (ICRA)*, pp. 3483–3488.
- Sun N, Fang Y, Zhang X, et al. (2012) Transportation task-oriented trajectory planning for underactuated overhead cranes using geometric analysis. *IET Control Theory & Applications* 6(10): 1410–1423.
- Wang K, Yan G, Ma G, et al. (2008) An earthworm-like robotic endoscope system for human intestine: design, analysis, and experiment. *Annals of Biomedical Engineering* 37(1): 210–221.

AQ5

AQ6

AQ7

AQ8

AQ9

AQ10

AQ11

AQ12

AQ13

Wang Q and Su C-Y (2006) Robust adaptive control of a class of non-linear systems including actuator hysteresis with Prandtl-Ishlinskii presentations. *Automatica* 42(5): 859–867.

Westervelt ER, Grizzle JW, Chevallereau C, et al. (2007) *Feedback Control of Dynamic Bipedal Robot Locomotion*. CRC Press.

Yamagata Y and Higuchi T (1995) A micropositioning device for precision automatic assembly using impact force of piezoelectric elements. In: *Proceedings, 1995 IEEE International Conference on Robotics and Automation*, 1995, pp. 666–671.

Yu H, Liu Y and Yang T (2008) Closed-loop tracking control of a pendulum-driven cart-pole underactuated system. *Proceedings of the Institution of Mechanical Engineers, Part I: Journal of Systems and Control Engineering* 222(2): 109–125.

Yu H, Huda M.N. and Wane SO (2011) A novel acceleration profile for the motion control of capsubots. In: *2011 IEEE International Conference on Robotics and Automation (ICRA)*, pp. 2437–2442.

AQ14**AQ15****AQ16**